

Data Matters: The Case of Predicting Mobile Cellular Traffic

Natalia Vesselinova, Matti Harjula and Pauliina Ilmonen
 Department of Mathematics and Systems Analysis, Aalto University, Finland
 {natalia.vesselinova, matti.harjula, pauliina.ilmonen}@aalto.fi

Abstract—Accurate predictions of base stations’ traffic load are essential to mobile cellular operators and their users as they support the efficient use of network resources and allow delivery of services that sustain smart cities and roads. Traditionally, cellular network time-series have been considered for this prediction task. More recently, exogenous factors such as points of interest and other environmental knowledge have been explored too. In contrast to incorporating external factors, we propose to learn the processes underlying cellular load generation by employing population dynamics data. In this study, we focus on smart roads and use road traffic measures to improve prediction accuracy. Comprehensive experiments demonstrate that by employing road flow and speed, in addition to cellular network metrics, base station load prediction errors can be substantially reduced, by as much as 56.5%. The code, visualizations and extensive results are available on <https://github.com/nvassileva/DataMatters>.

Index Terms—data, machine learning, mobile cellular traffic, forecasting, population dynamics.

I. INTRODUCTION

Accurate predictions of base stations’ (BSs) traffic load are essential to mobile cellular operators and their users as they support the efficient use of network resources and allow delivery of services that sustain smart cities and roads. Significant progress has been made in developing deep learning architectures for cellular traffic predictions [1]. Nonetheless, learning useful representations is generally based on mobile cellular key performance indicators (KPIs) much like it has been done in the past with classic statistical models for time-series predictions. Recent works incorporate exogenous information namely, auxiliary data about extrinsic factors that might have an effect on the cellular load [2]. Typically, these are points of interest (locations with high user activity). In some of the latest contributions [3], [4], the contextual description is enriched by including spatial, temporal and semantic relationships that describe the BSs and their surroundings.

In contrast to accounting for external factors, we propose to learn the intrinsic forces that govern the mobile cellular traffic generation. We hypothesize that by learning the processes underlying BS load generation, the accuracy with which cellular volume is predicted can be scaled up significantly. To this end we propose to employ data that characterizes population dynamics namely, the potential sources of cellular load and their fluctuations over time in addition to cellular KPIs.

The authors gratefully acknowledge the support received from Academy of Finland via the Centre of Excellence in Randomness and Structures, decision number 346308 and the computational resources provided by the Aalto Science-IT project.

TABLE I
 EMPLOYING POPULATION DYNAMICS IN ADDITION TO CELLULAR DATA
 IMPROVES PREDICTION PERFORMANCE BY AT LEAST 5.7% AND BY
 MORE THAN 50%

| BS # | MAE | | | MSE | | | MAPE | | | RMSE | | |
|---------|------|------|------|------|------|------|------|------|------|------|------|------|
| | min | mdn | max |
| 3054051 | 16.0 | 15.0 | 14.0 | 29.7 | 29.4 | 29.6 | 27.4 | 23.6 | 27.4 | 16.1 | 16.0 | 16.1 |
| 3086071 | 33.9 | 34.0 | 34.7 | 56.3 | 56.5 | 56.6 | 38.2 | 38.4 | 40.5 | 33.9 | 34.0 | 34.1 |
| 3086081 | 13.9 | 14.1 | 14.4 | 25.1 | 25.2 | 25.4 | 12.5 | 14.1 | 16.3 | 13.5 | 13.5 | 13.6 |
| 317706 | 16.6 | 16.4 | 15.0 | 33.8 | 33.2 | 33.5 | 15.8 | 13.7 | 18.7 | 18.6 | 18.3 | 18.4 |
| 317715 | 8.0 | 8.4 | 7.8 | 14.0 | 13.3 | 11.1 | 15.6 | 15.4 | 20.8 | 7.3 | 6.9 | 5.7 |
| 320280 | 18.3 | 18.4 | 27.4 | 35.3 | 36.8 | 40.0 | 12.5 | 12.5 | 14.3 | 19.6 | 20.5 | 22.5 |
| 320287 | 23.0 | 21.4 | 19.5 | 38.9 | 36.8 | 35.1 | 25.5 | 23.5 | 23.4 | 21.8 | 20.5 | 19.4 |
| 3410061 | 12.5 | 12.0 | 12.0 | 20.6 | 20.9 | 20.6 | 30.4 | 31.9 | 33.6 | 10.9 | 11.0 | 10.9 |

^aMean Absolute (Percentage) Error (MA(P)E), (Root) Mean Square Error ((R)MSE).

^bThe three values listed per error type are the minimum, median and maximum.

We focus on highways and teleoperated and autonomous driving; hence, on short-term forecasting, which is arguably more challenging than mid- and long-term but relevant to low-latency and high-reliability services, especially those related to smart traffic and vehicles. We combine road data with mobile cellular KPIs to enrich the cellular time-series with population dynamics data. The computational cost of using road statistics is negligible, especially compared to recent studies [3], which incorporate a large knowledge graph. The combined improvement attained from using this graph and the developed deep learning architecture in [3] when contrasted with state-of-the-art approaches is at most 18% [3]. In our study, we record improvements above 50%, Table I, due to the use of road statistics alone. The communication overhead between BSs and roadside units, which are typically used in smart roads where real-time traffic statistics are within reach, is of little relevance.

Our primary contributions are:

- We are the first to propose and capture the phenomena intrinsic to mobile cellular traffic generation. We employ road traffic metrics to gauge the potential sources of BS load in highways together with cellular time-series. This leads to substantial improvements in prediction accuracy.
- We develop a methodology for generating cellular traffic volumes in highways based on real-life road traffic data.
- We conduct comprehensive experiments for a real-world highway under quickly fluctuating road traffic load, seasonal changes and a diversity of mobile communication volumes, which complement our first study [5].

- We examine highways and address short-term mobile cellular traffic predictions in contrast to the extensively studied urban scenario and long-term cellular forecasting.

The methodology we develop for creating cellular traffic data sets based on road traffic is explained in Section II. A description of the real highway scenario used in the experiments can be found in Section III. The traffic prediction problem and the implemented learning model are formulated in Section IV. We discuss the experimental setting, methodology and protocol, and performance results in Section V. The novelty and impact of the approach we propose are highlighted in Section VI. The main results and future prospects are summarized in Section VII. The code, extensive results and visualizations are available on <https://github.com/nvassileva/DataMatters>.

II. METHODOLOGY

Measuring and recording a large variety of different KPIs is intrinsic to any communication network because the measurements are used for monitoring, operating, optimizing and maintaining the network. However, mobile operators rarely share such data because of privacy concerns. One of the very few open access data sets [6] is the Telecom Italia Big Data Challenge [7]. Therefore, the majority of the studies, which develop machine learning methods for predicting mobile cellular traffic, routinely use it [2]. Commonly, their goal is to predict the number of calls as a measure of the cellular network load. We adopt the same approach of using the total calls number as BS load indicator too—we expect the general trends we observe in this study to remain the same independent of the load traffic measure used.

Similar to the KPIs' relevance to mobile cellular networks, road traffic measurements are critical to any off-the-shelf traffic management system. In contrast to cellular KPIs, however, traffic measurements are open access. The California Department of Transportation (Caltrans), for instance, is maintaining a Performance Measurement System (PeMS) [8] with real-time traffic data from a large number of individual detectors deployed statewide in the California freeway system. Both real-time and historical measurements are freely available.

We use real-life PeMS data to generate mobile cellular traffic due to the lack of open data sets comprising both network KPIs and road traffic measurements. Before describing our methodology, we summarize the variables we use from PeMS.

A. Road data

The road metrics employed in this study are *vehicular flow*—the number of vehicles that pass by a specific location during a time interval—and *speed* of the flow. In the PeMS data set, the former metric is aggregated over five-minute intervals and the latter is averaged over these intervals.

We make an important assumption that road traffic is measured outside yet in the vicinity of the BS of interest, so that the flow and speed measured in time slot t are observed during time slot $t + 1$ in the area covered by this BS.

B. Mobile cellular data generation

We use the described PeMS variables to emulate the time of arrival of the vehicles per five-minute time slot, the dwell time they spent in the cell and their departure times. These, together with the call duration, are then used to determine if a call is handed over to the next BS on the road or if it is terminated before the vehicle leaves its serving BS.

1) *Vehicular flow arrival and departure*: The loop detectors of the Caltrans system measure all variables in real time yet the measurements are recorded in PeMS as aggregates for the number of vehicles and as averages for the speed per five-minute intervals, as mentioned earlier. Vehicular arrival and departures times at a BS are needed to simulate the call cellular load. The classic Poisson assumption about arrival times has been validated in [9] with real data from highways for sparse—not congested nor experiencing bursts—traffic. Since for the large majority of the data we employ, the speed is around its maximum allowed value, suggesting congestion is not habitual, we adopt this assumption too. In effect, we emulate each vehicle's arrival time by exponential inter-arrival times within each five-minute interval. The vehicle's departure time is determined by its arrival and cell dwell times.

2) *Dwell time*: The time spent by a vehicle in a segment of a highway served by a BS, is modeled by the BS's range and the measured PeMS average speed. We add Gaussian noise with mean zero and standard deviation 0.05 to emulate different speeds.

3) *Calls*: New call arrivals at a BS follow a Poisson process as demonstrated empirically, analytically and by simulation [10]. Therefore, we model the calls placed by each vehicle by exponential call inter-arrival times. Each vehicle generates calls with a given rate λ , common for all vehicles. Although λ is fixed, the new call arrival process at a BS is a non-homogeneous Poisson process, with time-varying arrival rate given by the sum of the time-varying vehicular arrival rate (different per five-minute interval) and the fixed call arrival rate. As this is a random process, each passing vehicle might generate no service request, at most one, or multiple requests while driving through the segment of the freeway covered by the BS. Furthermore, during congestion periods, the simulated load on the network grows correspondingly (see Section V-A2).

We do not model the handover arrival process explicitly. The number and rate of handovers are determined by the start and end times of the simulated calls and the vehicle's departure time from a BS. Hence, the handover process is completely defined by the call duration, cell range, vehicle's speed and new call generation process. If the call is not terminated before the vehicle's departure time, it is transferred to the next BS. Since we do not model the service capacity of a BS, all calls are accepted by the BS and correspondingly, counted.

4) *Call duration*: Call duration has been traditionally modeled by the exponential random variable [10]. However, more recent field studies show that a better fit for the call duration distribution might be the log-normal distribution [11] or a mixture of two log-normal distributions [12]. The latter can

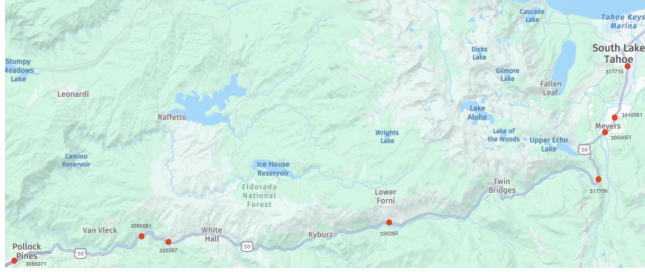


Fig. 1. A map of the section of US50-E El Dorado County freeway used in the study (in gray). The red dots indicate the approximate location of the PeMS detectors on that segment, from Pollock Pines to Lake Tahoe Airport. A larger image is available on <https://github.com/nvassileva/DataMatters>.

model diurnal (longer) and nocturnal (shorter) calls [13] or a mixture of two different services, for instance.

5) *Flow between adjacent cells*: The vehicular flows in two adjacent BSs can differ from each other. The recorded number of vehicles in one segment of the highway can be smaller or higher than that of the subsequent segment. This can be due to arterial roads that merge into the highway. When the incoming flow in the target cell is smaller than the outgoing flow from the preceding cell, we randomly remove vehicles together with their corresponding handover calls from the generated data set. The goal is to reflect the route deviation of the vehicles, namely those that leave the highway, into the network statistics too. When the flow in the target cell is larger than the adjacent, preceding cell, no adjustments are made in the handover statistics generated in the preceding cell.

III. A HIGHWAY SCENARIO

We consider a sector of the US50-E freeway in El Dorado County, California; specifically, the one shown in Figure 1. The Caltrans detectors, whose measurements are used in the study, are listed in Table II in sequential order together with the distance between each two consecutive detectors.

The density of the PeMS detectors is high at the fragments of the highway that cross populated areas (such as villages and towns; Pollac Pines and Mevers in this particular scenario) and is much lower on the highway sectors of mountainous regions. Long-range BS typically cover rural areas with sparse population, whereas short-range BSs provide coverage in densely populated (urban) regions. Since the density of the road detectors seems to be guided by similar principles—long-term density of the vehicular traffic—as the placement of BSs—population density and the particularities of the terrain—we choose the range of the BSs to match the distance between sensors. This provides us with a variety of diverse use cases. The road segments exhibit different capacity, average vehicular density and propensity for congestion, which conditions together with the different BSs' ranges model dynamic, time- and location-varying call volumes. For simplicity, we make the assumption that the vehicular traffic is unidirectional, flowing from Pollac Pines to South Lake Tahoe.

TABLE II
PEMS US50-E DETECTORS USED IN THE STUDY
AND THE DISTANCE BETWEEN CONSECUTIVE ONES.
BSS HAVE THE SAME ID AS THE SENSORS.

| PeMS detectors | miles |
|---|-------|
| Mainline VDS 3086071–50EB JWO Sly Park EB | 7.67 |
| Mainline VDS 3086081–50EB at Riverton Barn CCTV | 1.62 |
| Mainline VDS 320287–50EB At Ice House | 13.27 |
| Mainline VDS 320280–Wrights Lake Rd | 13.41 |
| Mainline VDS 317706–Echo Summit | 3.89 |
| Mainline VDS 3054051–50EB into Luther 50/89 R. | 0.99 |
| Mainline VDS 3410061–50EB JEO Pioneer Trl | 3.22 |
| Mainline VDS 317715–F St | 1.46 |

IV. MOBILE CELLULAR TRAFFIC PREDICTION: DEFINITION AND SOLUTION

We assess the efficacy of our proposed approach by training a suitable machine learning model with historical cellular data *together with* versus *without* incorporating road traffic data. The classic machine learning model we implement is individually trained (with the BS's own data) for each BS along the highway.

A. Problem Formulation

Mathematically, we denote by $\mathbf{x}^\tau \in \mathcal{R}^p$ a random variable comprising historical measurements of p metrics relevant to a given cell: cellular traffic volume or cellular and road traffic volume and speed measurements. Given a time sequence of M such historical observations $\{\mathbf{x}^{\tau-M+1}, \dots, \mathbf{x}^\tau\}$, our objective is to learn a prediction model \mathcal{F} that can forecast the future mobile traffic load \hat{x} in the cell during the next time step:

$$\hat{x}^{\tau+1} = \mathcal{F}(\mathbf{x}^{\tau-M+1}, \dots, \mathbf{x}^\tau), \quad (1)$$

so that the prediction error is minimized:

$$\min L(\hat{x}, x),$$

where the loss function $L(\cdot)$ measures the difference between the estimated \hat{x} and observed x mobile cellular traffic.

B. A classic machine learning model

Mobile cellular traffic volumes at BSs experience spatial-temporal dependencies. Since we focus on a short-term forecasting problem at a BS (1), the impact of correlations is confined to the adjacent BSs. We account for this phenomenon by the incoming vehicular flow and speed.

The classic long short-term memory (LSTM) model has been broadly applied to time-series prediction tasks either as a singular learning structure or as a basic component of more complex models. Furthermore, LSTM has been shown to excel in very short-term cellular forecasting [14], which motivates our choice.

The model we construct is composed by an LSTM layer, followed by a fully connected feedforward neural network (a multilayer perceptron). This dense layer consists of a single unit and no activation function. It is a linear transformation

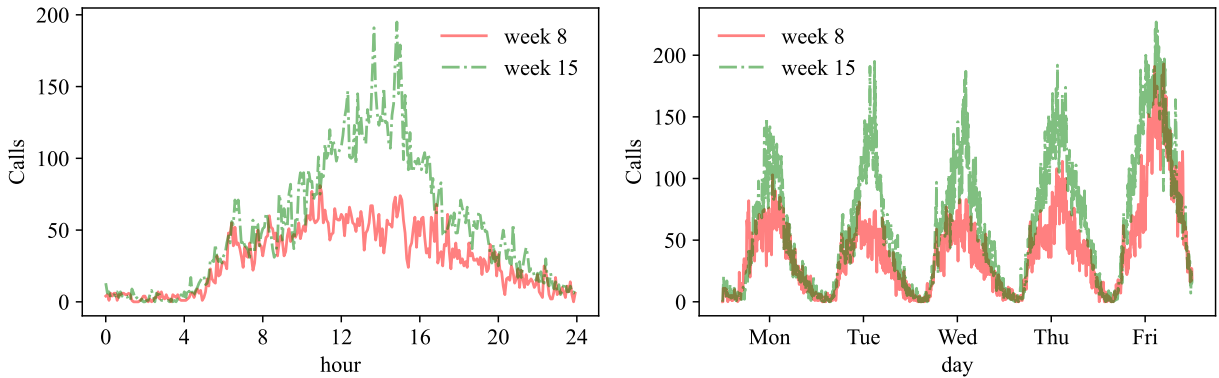


Fig. 2. BS 320287 Tuesday's and weekly fluctuations of cellular load for two specific weeks.

that maps the final LSTM state into a single target value—the estimated number of calls in a BS.

Mathematically, the model can be represented as two functions $f(g)$, where $g(\cdot)$ is the LSTM learning structure, which transforms the input data into new features. The representation function $f(\cdot)$ maps the learned features into a cellular traffic load prediction for the BS under consideration.

V. EXPERIMENTS AND RESULTS

A. Setting

1) *Input variables' values*: Real road traffic data from Caltrans detectors of the US50-E highway in El Dorado County, California are used in the experiments. The considered time period is 24-week-long, from March 28, 2022 to September 9, 2022 (week 13 to week 36 of 2022). The data comprise the flow and speed from Monday to Friday of each week. There are 288 data points per day due to the 5-minute granularity.

We generate the network statistics following the methodology developed in Section II and input values as follows. New calls are generated with arrival rate $\lambda = 1/5$, one call per 5-minute interval on average. When defining the mean call duration and its variance, we are guided by [13] and [11]. We set the mean call duration to 1 and 10 minutes for a mixture of two log-normally distributed calls, each with equal weight. The variance of the log-normal calls is 3 times larger than their mean [13]. The range of the BSs is listed in Table II.

2) *Data*: All BSs experience a highly dynamic road and cellular traffic volumes. The period from March to September accounts for different seasons and correspondingly, diverse road traffic patterns that reflect seasonal changes and holiday periods. As a result, each BS has different daily and weekly profiles along the studied period. Furthermore, for all BSs the flow and communication load vary quickly within the 5-minute intervals. Figure 2 shows the profile of call load 1) for the same location and day of a week but different weeks and 2) for all work days of a week and different weeks for a BS as an example.

The correlation between the road metrics—flow and speed—varies greatly between segments of the highway and

with time: strongly inverse, reciprocal or lacking linear association. This variability can be explained by the flow-speed correlation dependence on the capacity of the road segment, vehicular flow, terrain, location and time.

Flow and the generated number of calls are strongly correlated. This reciprocal linear association, corresponds to recent [15] and earlier studies [16], which show that there exists a strong correlation between population density and mobile cellular use in urban scenarios. Research on population mobility, in effect, relies on such a high correlation when using call detail records from mobile operators to understand and model human mobility in urban environments [17]. Furthermore, people's density is often estimated from mobile phone network data [17], [18]. Under the assumption of connected vehicles and a highway scenario—the setting of our study—the load on the BSs that serve the highway is exclusively generated by the road traffic on that highway (services used by the autonomous driving vehicles and their passengers). Naturally, the highest correlation is between the flow of vehicles and the new calls they place on their serving BS and correspondingly, the total number of calls. The correlation between the flow and number of handovers is often of a smaller magnitude as not all vehicles have active calls when crossing the borders between BSs, namely when arriving to a new cell.

The number of calls is in general inversely related to the speed as whenever the road is congested, the dwell time of the vehicle on the road is increased and consequently the probability of initiating a new call grows. This is in line with the common observation that the load on the mobile cellular network increases during traffic jams.

3) *Machine learning model*: Our model has a single LSTM layer with 16 cells. In the training phase, we use the root mean square propagation and mean squared error (MSE) loss for optimizing the models parameters. We set the length of the historical traffic series to six samples (30 min) due to the speed with which changes in the traffic volume occur in 5-minute intervals. The prediction horizon is the next 5-minute interval. The 24 weeks of data are split 12:6:6 chronologically into training, validation, and testing after which data are shuffled.

B. Evaluation methodology and protocol

Since our goal is to assess the effectiveness of employing data intrinsic to mobile cellular volume generation, we contrast the prediction performance of the implemented machine learning model when cellular KPIs are used (the baseline) with the model's performance when these same data are enriched with vehicular flow and speed metrics. We evaluate the predictions over a comprehensive set of highway and cellular conditions. Similar methodology of assessing the impact of data on prediction accuracy is followed in [19] when examining the efficacy of incorporating an urban knowledge graph.

We measure the forecasting performance with the mean absolute error (MAE), mean absolute percentage error (MAPE), MSE and root mean squared error (RMSE). To have a common basis for comparison and to fairly attribute the performance deviation to the data set employed in learning, we train and evaluate the model with the same hyper-parameters Section V-A3 using data from the same period and location but with different features: either containing purely network metrics or a set of network and road traffic metrics. We measure the improvement in prediction as the percentage difference in error by $(ErrM_{net} - ErrM_{net\&road})/ErrM_{net}$, where $ErrM$ is the error measure.

C. How much can population dynamics data help?

1) *Overall performance:* Comprehensive results from the four different data sets—1) calls (denoting total number of calls, that is, the sum of new and handover calls) only; 2) flow, speed and calls; 3) new, handover, calls and 4) flow, speed, new, handover, calls—when the call duration is modeled by a mixture of two log-normal distributions are summarized in Table III and Table IV. For each error metric we show the minimum, median and maximum of the 5 simulation runs conducted for each data set and BS. We make the observations as follows:

- **Employing data that captures the processes intrinsic to mobile cellular traffic generation consistently improves cellular load prediction performance.** All BSs observe improvements in all their forecasting measures when learning from both network and road traffic data.

The prediction error reduction among all BSs is between 8.4% and 33.9% (MAE), 13.3% and 56.5% (MSE), 12.5% and 38.4% (MAPE), and 6.9% and 34% (RMSE) when in addition to (total number of) calls, also flow and speed are employed, and when comparing the medians of all BSs, see Figure 3 (left). Similar improvement trends are recorded for the minimum and maximum errors, Table I. Using more refined network KPIs—those that contain the number of new and handover calls, and their total—and road data, reduces the prediction errors too: between 7.5% and 21.8% (MAE), 11% and 35.4% (MSE), 10.9% and 25.7% (MAPE), and 5.7% and 19.7% (RMSE) for the medians, see Figure 3 (right), and likewise for the smallest and largest errors.

- **Road traffic metrics can capture the processes underlying mobile cellular load generation.** We employ

flow and speed as a means to characterize the underlying population dynamics in highways and through them the data generation process. The flow captures the number of potential call generation sources. The speed can indicate density dynamics and can also serve as a gauge for road traffic congestion and hence, for increased load on the BS. The number of handovers (or equivalently, the handover rate) is an indicator of mobility too yet our results are not conclusive about its impact. Contrasting the performance of calls to that of new, handover, and calls, we observe an error improvement in some of the error measures: it is in the order of no more than 3% for the majority of the BSs, see Figure 4 (left and center plots).

Finally, employing flow, speed and calls (3 variables) leads to a large reduction in the prediction errors even when contrasted with employing new, handover and calls (3 variables): 8.6% and 22.8% (MAE), 14.2% and 36.3% (MSE), 11.5% and 25% (MAPE), and 7% and 20.2% (RMSE) for the medians, Figure 4 (right plot).

- **Choice of data (split) and hyper-parameter tuning.** The shown results are from using 24 weeks of data and 75:25 ratio of train and validation to test data. We observed cases when the performance of some of the BSs is decreased when using road data. This is the case for the MSE and RMSE of BS 320287 when the data set consists of weeks 15 to 21 and the data is chronologically split into 3:2:2 for training, validation and testing¹. We identify week 15 as outlying from the other training weeks and consequently, as the main explanation for the results. For the same period but with 4:1:2 partition of the data, the results are consistent with what we report above—decreased prediction errors across all performance measures and BSs when employing flow and speed time-series in addition to call time-series data. This 4:1:2 data split also turns into smaller forecasting errors for the purely network data sets. In other words, choice of data that captures the underlying patterns and an appropriate hyper-parameter tuning are always required. In our on-going work we are studying the effect of the data split on the overall forecasting performance.

- 2) *Sensitivity to road metrics accuracy:* We envision that road traffic measurements can directly be fed into the learning algorithms as smart cities and roads are equipped with detectors that can provide such critical information. Another alternative is to use road traffic predictions instead of measurements. The machine learning research community has seen a surge of deep learning methods that tackle this prediction task with several solutions that achieve high levels of forecasting accuracy [20].²

¹See <https://github.com/nvassileva/DataMatters> for detailed results.

²An advantage of such an approach is that the mobile cellular prediction algorithms can receive in advance information about the vehicular flow and speed that will be evidenced in the BS during the next time slot. This timely received data can increase further the prediction accuracy of the algorithms. In fact, our preliminary results validate this concept under similar conditions as those we report above.

TABLE III
PREDICTION PERFORMANCE ON CALLS DATASET AND FLOW, SPEED AND CALLS DATASET

| BS | Calls | | | | | | | | | | | | Flow Speed Calls | | | | | | | | | | | |
|---------|-------|-------|-------|-------|-------|-------|-------|-------|-------|-------|-------|-------|------------------|-------|-------|-------|-------|-------|-------|-------|-------|-------|-------|-------|
| | MAE | | | MSE | | | MAPE | | | RMSE | | | MAE | | | MSE | | | MAPE | | | RMSE | | |
| | min | mdn | max | min | mdn | max | min | mdn | max | min | mdn | max | min | mdn | max |
| 3054051 | 0.434 | 0.434 | 0.439 | 0.485 | 0.492 | 0.503 | 116.0 | 118.0 | 128.3 | 0.697 | 0.702 | 0.709 | 0.364 | 0.369 | 0.377 | 0.341 | 0.347 | 0.354 | 84.3 | 90.1 | 93.1 | 0.584 | 0.589 | 0.595 |
| 3086071 | 0.282 | 0.283 | 0.287 | 0.154 | 0.155 | 0.157 | 820.8 | 837.2 | 880.6 | 0.392 | 0.393 | 0.396 | 0.187 | 0.187 | 0.187 | 0.067 | 0.067 | 0.068 | 506.8 | 515.6 | 523.9 | 0.259 | 0.259 | 0.261 |
| 3086081 | 0.394 | 0.396 | 0.399 | 0.317 | 0.318 | 0.319 | 335.2 | 347.4 | 365.4 | 0.563 | 0.564 | 0.565 | 0.339 | 0.34 | 0.342 | 0.237 | 0.238 | 0.238 | 293.2 | 298.3 | 305.9 | 0.487 | 0.487 | 0.488 |
| 317706 | 0.155 | 0.156 | 0.158 | 0.058 | 0.059 | 0.060 | 127.5 | 128.4 | 137.8 | 0.241 | 0.242 | 0.244 | 0.129 | 0.13 | 0.135 | 0.038 | 0.039 | 0.040 | 107.4 | 110.8 | 112.0 | 0.196 | 0.198 | 0.199 |
| 317715 | 0.321 | 0.324 | 0.325 | 0.242 | 0.243 | 0.246 | 103.5 | 109.3 | 117.3 | 0.492 | 0.493 | 0.496 | 0.295 | 0.297 | 0.3 | 0.208 | 0.21 | 0.218 | 87.4 | 92.4 | 92.8 | 0.456 | 0.459 | 0.467 |
| 320280 | 0.080 | 0.081 | 0.097 | 0.013 | 0.013 | 0.015 | 54.0 | 54.6 | 57.3 | 0.112 | 0.114 | 0.121 | 0.065 | 0.066 | 0.070 | 0.008 | 0.008 | 0.009 | 47.3 | 47.7 | 49.1 | 0.090 | 0.091 | 0.094 |
| 320287 | 0.066 | 0.067 | 0.067 | 0.009 | 0.009 | 0.009 | 86.7 | 87.0 | 88.3 | 0.094 | 0.094 | 0.094 | 0.051 | 0.052 | 0.054 | 0.005 | 0.006 | 0.006 | 64.6 | 66.6 | 67.7 | 0.073 | 0.075 | 0.076 |
| 3410061 | 0.404 | 0.404 | 0.407 | 0.389 | 0.391 | 0.397 | 696.4 | 725.7 | 757.9 | 0.624 | 0.626 | 0.63 | 0.354 | 0.356 | 0.358 | 0.309 | 0.31 | 0.316 | 484.8 | 494.5 | 503.2 | 0.556 | 0.557 | 0.562 |

^aThe three values listed per error type are the minimum, median and maximum. The MAPE values are in percentage.

TABLE IV
PREDICTION PERFORMANCE ON NEW, HANDOVER, AND TOTAL CALLS DATASET AND THE SAME DATASET BUT ENRICHED WITH FLOW AND SPEED TIME-SERIES

| BS | New HO Calls | | | | | | | | | | | | Flow Speed New HO Calls | | | | | | | | | | | |
|---------|--------------|-------|-------|-------|-------|-------|-------|-------|-------|-------|-------|-------|-------------------------|-------|-------|-------|-------|-------|-------|-------|-------|-------|-------|-------|
| | MAE | | | MSE | | | MAPE | | | RMSE | | | MAE | | | MSE | | | MAPE | | | RMSE | | |
| | min | mdn | max | min | mdn | max | min | mdn | max | min | mdn | max | min | mdn | max | min | mdn | max | min | mdn | max | min | mdn | max |
| 3054051 | 0.426 | 0.428 | 0.431 | 0.479 | 0.498 | 0.504 | 101.3 | 103.1 | 114.5 | 0.692 | 0.706 | 0.71 | 0.366 | 0.369 | 0.37 | 0.343 | 0.35 | 0.355 | 83.7 | 88.2 | 91.9 | 0.585 | 0.591 | 0.596 |
| 3086071 | - | - | - | - | - | - | - | - | - | - | - | - | - | - | - | - | - | - | - | - | - | - | - | - |
| 3086081 | 0.39 | 0.39 | 0.392 | 0.307 | 0.307 | 0.309 | 326.7 | 337.1 | 349.7 | 0.554 | 0.554 | 0.556 | 0.336 | 0.339 | 0.346 | 0.235 | 0.235 | 0.238 | 294.6 | 300.3 | 321.9 | 0.484 | 0.485 | 0.488 |
| 317706 | 0.154 | 0.155 | 0.158 | 0.056 | 0.057 | 0.06 | 128.1 | 131.7 | 134.0 | 0.237 | 0.24 | 0.245 | 0.131 | 0.131 | 0.133 | 0.039 | 0.04 | 0.041 | 106.6 | 112.0 | 114.1 | 0.199 | 0.2 | 0.202 |
| 317715 | 0.323 | 0.326 | 0.329 | 0.242 | 0.245 | 0.25 | 106.3 | 111.3 | 113.4 | 0.492 | 0.495 | 0.5 | 0.299 | 0.304 | 0.306 | 0.215 | 0.218 | 0.233 | 82.2 | 85.5 | 91.9 | 0.463 | 0.467 | 0.482 |
| 320280 | 0.076 | 0.081 | 0.100 | 0.012 | 0.012 | 0.015 | 54.0 | 55.5 | 56.4 | 0.108 | 0.111 | 0.123 | 0.062 | 0.063 | 0.069 | 0.008 | 0.008 | 0.008 | 44.9 | 46.8 | 48.6 | 0.087 | 0.089 | 0.092 |
| 320287 | 0.066 | 0.066 | 0.067 | 0.009 | 0.009 | 0.009 | 87.8 | 88.7 | 90.6 | 0.093 | 0.094 | 0.094 | 0.052 | 0.053 | 0.055 | 0.005 | 0.006 | 0.006 | 65.5 | 66.0 | 70.4 | 0.073 | 0.075 | 0.078 |
| 3410061 | 0.405 | 0.408 | 0.415 | 0.394 | 0.403 | 0.423 | 590.1 | 639.2 | 655.4 | 0.628 | 0.635 | 0.65 | 0.355 | 0.357 | 0.363 | 0.312 | 0.316 | 0.322 | 458.7 | 474.7 | 483.2 | 0.558 | 0.562 | 0.568 |

^aBS 3086071 is the first one in our scenario. Therefore, there is no handover traffic from a preceding BS.

TABLE V
PREDICTION PERFORMANCE WITH GAUSSIAN NOISE ADDED TO THE FLOW

| BS | Flow Speed Calls | | | | | | | | | | | | Flow Speed New HO Calls | | | | | | | | | | | |
|---------|------------------|-------|-------|-------|-------|-------|-------|-------|-------|-------|-------|-------|-------------------------|-------|-------|-------|-------|-------|-------|-------|-------|-------|-------|-------|
| | MAE | | | MSE | | | MAPE | | | RMSE | | | MAE | | | MSE | | | MAPE | | | RMSE | | |
| | min | mdn | max | min | mdn | max | min | mdn | max | min | mdn | max | min | mdn | max | min | mdn | max | min | mdn | max | min | mdn | max |
| 3054051 | 0.369 | 0.371 | 0.375 | 0.348 | 0.354 | 0.358 | 84.0 | 85.9 | 87.8 | 0.59 | 0.595 | 0.598 | 0.367 | 0.368 | 0.372 | 0.343 | 0.348 | 0.354 | 86.3 | 89.4 | 92.7 | 0.586 | 0.589 | 0.595 |
| 3086071 | 0.205 | 0.205 | 0.206 | 0.077 | 0.077 | 0.078 | 594.5 | 599.4 | 602.1 | 0.278 | 0.278 | 0.279 | - | - | - | - | - | - | - | - | - | - | - | - |
| 3086081 | 0.346 | 0.349 | 0.35 | 0.244 | 0.245 | 0.247 | 293.1 | 315.5 | 320.6 | 0.494 | 0.495 | 0.497 | 0.344 | 0.347 | 0.348 | 0.241 | 0.242 | 0.243 | 311.9 | 314.9 | 315.8 | 0.491 | 0.492 | 0.493 |
| 317706 | 0.134 | 0.136 | 0.138 | 0.04 | 0.042 | 0.043 | 110.0 | 111.3 | 119.5 | 0.2 | 0.205 | 0.207 | 0.135 | 0.135 | 0.138 | 0.041 | 0.042 | 0.043 | 107.5 | 110.8 | 117.1 | 0.202 | 0.204 | 0.207 |
| 317715 | 0.301 | 0.303 | 0.306 | 0.214 | 0.214 | 0.224 | 88.5 | 91.0 | 96.4 | 0.462 | 0.463 | 0.473 | 0.303 | 0.304 | 0.309 | 0.216 | 0.22 | 0.228 | 89.7 | 94.0 | 95.6 | 0.465 | 0.469 | 0.477 |
| 320280 | 0.070 | 0.072 | 0.074 | 0.009 | 0.009 | 0.010 | 50.5 | 50.9 | 51.1 | 0.096 | 0.097 | 0.098 | 0.071 | 0.076 | 0.084 | 0.009 | 0.010 | 0.011 | 49.8 | 50.0 | 52.1 | 0.095 | 0.099 | 0.104 |
| 320287 | 0.057 | 0.057 | 0.058 | 0.006 | 0.006 | 0.006 | 71.7 | 72.9 | 74.8 | 0.079 | 0.080 | 0.080 | 0.056 | 0.057 | 0.058 | 0.006 | 0.006 | 0.007 | 72.9 | 75.0 | 76.4 | 0.078 | 0.079 | 0.083 |
| 3410061 | 0.36 | 0.361 | 0.365 | 0.313 | 0.318 | 0.327 | 481.2 | 495.0 | 514.7 | 0.56 | 0.564 | 0.572 | 0.361 | 0.362 | 0.369 | 0.32 | 0.322 | 0.334 | 475.7 | 496.3 | 510.8 | 0.566 | 0.567 | 0.578 |

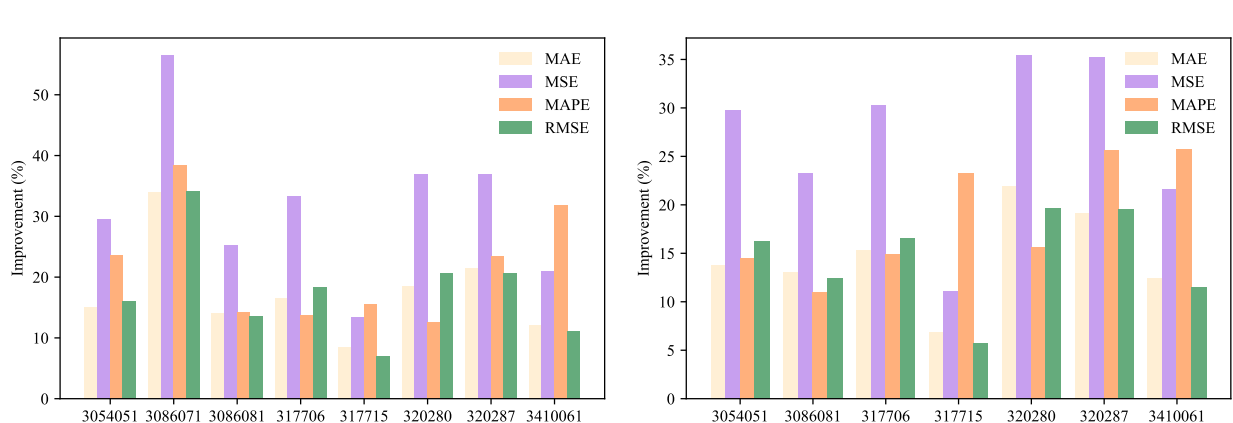


Fig. 3. Improvement in prediction when employing (left) calls vs calls, flow and speed data and (right) new, handover and total number of calls vs the same data set enriched with flow and speed statistics.

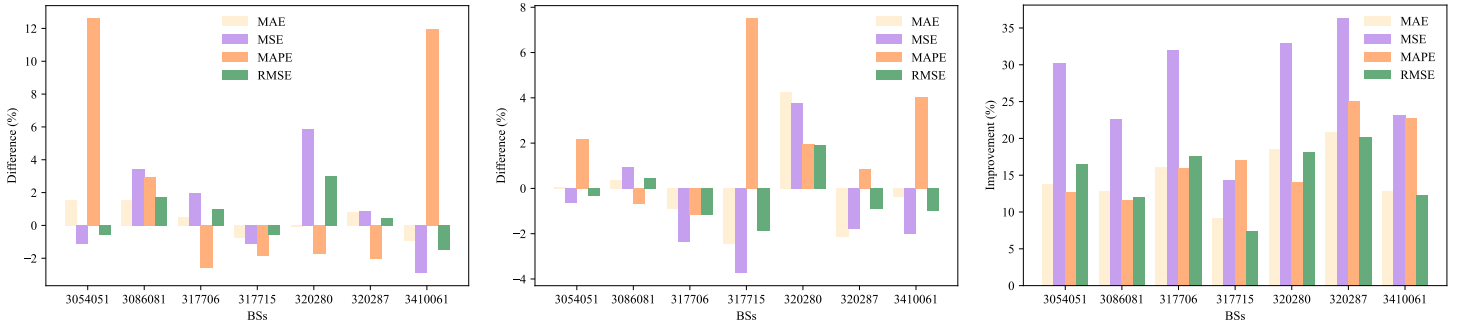


Fig. 4. Prediction error reduction when contrasting: **(left)** calls (baseline) vs the same data (C) augmented with new, handover and calls (NHC); **(center)** flow, speed, calls (FSC) (baseline) vs flow, speed, new, handover and total number of calls (FSNHC). **(right)** NHC data set (baseline) vs FSC.

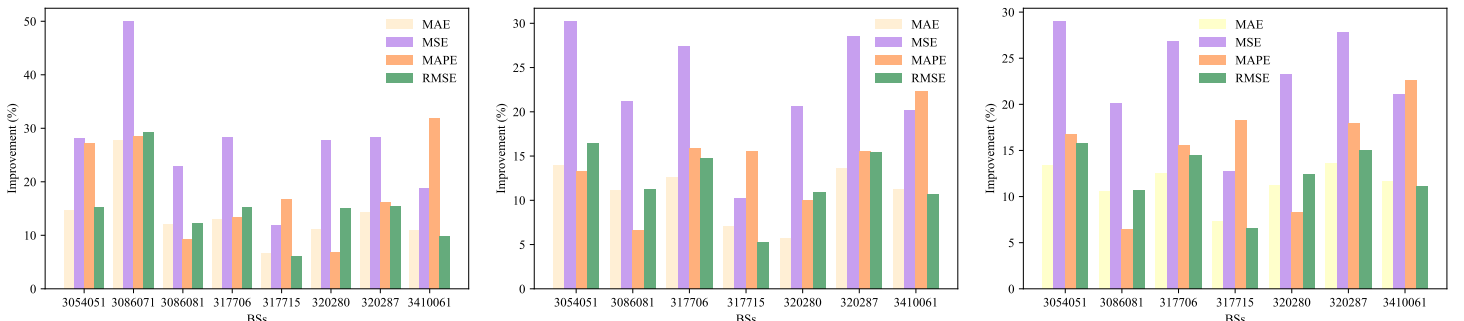


Fig. 5. Improvement in prediction when the flow is estimated with errors. Contrasting: **(left)** calls (baseline) vs the same data (C) augmented with vehicular flow estimated with errors and speed (\hat{F} SC); **(center)** NHC (baseline) vs \hat{F} SNHC. **(right)** NHC (baseline) vs \hat{F} SC.

To assess the sensitivity of the mobile cellular predictions to estimation errors in the road predictions, we introduce an estimation error in the flow measurements by the PeMS detectors. In particular, we assume a prediction error of 5% in the number of vehicles per 5-minute intervals, modeled by adding Gaussian noise to the real PeMS measurements:

$$\hat{v} = v + \epsilon, \quad \epsilon \sim \mathcal{N}(0, \sigma), \quad (2)$$

where v denotes the real PeMS flow data and \hat{v} is the estimated flow. Whereas our learning model is fed with the estimated value of the flow variable \hat{v} , we generated the mobile cellular traffic load with the true PeMS measurement v .

The results are reported in Table V and show that although the noise in the flow variable decreases cell load prediction accuracy, employing road data is largely beneficial yet. Overall, across all error measures and all BSs and the 4 data sets, the prediction error improvement is between 5.2% and 49.9%, Figure 5 (left and center plots), for the medians when using estimated (namely, with errors) road traffic time-series data.

Employing flow, speed and calls—when flow is reported with errors—leads to a reduction in the prediction errors even when contrasted with new, handover and calls data set: the improvement is between 6.4% and 29% for the medians among the MAE, MAPE, MSE, and RMSE error measures, Figure 5 (right plot).

VI. NOVELTY AND IMPACT

Novelty. Mobile cellular load forecasting is native to network resource optimization and delivery of services with reliability, latency and quality guarantees. Therefore, it has remained prominent across all generations of communication networks. In the latest research in this area, the primary focus is on developing larger and more powerful machine learning models [1], [2]. When it comes to data, the state-of-the-art contributions (see [2] for an overview) focus on incorporating exogenous information. In particular, these studies rely on environmental data—in addition to cellular time-series—as such auxiliary information describes the BS context and can bring improvements in terms of reduced prediction errors [3], [4]. A few deep learning algorithms [21], [22] explicitly incorporate handover rates between BSs in an attempt to better reflect traffic fluctuations via user mobility. Nonetheless, none of the prior art proposals explores data that can implicitly or explicitly characterize the data sources and their variability. The novelty of our approach consists of modeling the internals of the cellular traffic generation phenomenon. We do this by counting the potential sources of cellular traffic and by accounting for their velocity.

Impact. Employing population dynamics has the potential not only to reduce the uncertainty about future cellular volumes but also to reduce the cost of collecting big and diverse data and hence, to reduce the computational complexity and

memory requirements and ultimately, to decrease the energy expenditure too. Lighter learning models are also more versatile as they can be used at the edge and in roadside units too. Furthermore, concept drift [1] arising from changes in network configurations or conditions and users' behavior would have a major impact on models relying on knowledge graphs as these graphs would need to be updated first.

Potential limitations. The concept of employing population dynamics together with relevant mobile cellular data to accurately predict cellular traffic is of a much broader scope than a specific scenario. We validate our idea in a highway scenario yet we conjecture that it is applicable to the urban setting too. At present, a limitation for the implementation of our idea in practice is the potential lack of real-time population density and mobility data. Currently, real-time road traffic measurements are an integral part of the urban transportation management systems and these can be used in forecasting the service load placed by vehicles and their passengers on the cellular network. In the future, different means for estimating pedestrian density will be available too. The application of optical cables for simultaneous data transmission and tracking of people in a train station, for instance, is discussed in [23].

VII. CONCLUSION

Mobile cellular data have been used to model population dynamics with the aim to better understand urban mobility. We take a different look and employ population dynamics in a highway to forecast mobile cellular traffic on the highway. Our contributions stem from proposing the type of data that can, in practice, substantially scale up the accuracy of mobile cellular traffic predictions. In particular, we propose to employ data that characterizes the sources of communication volume and its dynamics in addition to BS traffic load.

We validate our hypothesis in a real highway scenario by using vehicular flow and speed time-series. The results show that the traffic load prediction error at each BS can be largely and consistently reduced: between about 5% and 56.5% depending on the error measure, BS and specific data sets. These results are obtained for BSs featuring realistic conditions including different range, fluctuating road traffic and cellular volumes.

We sincerely hope that this powerful result will prompt future research. Our proposal can boost the prediction accuracy of centralized and distributed learning models for short-, mid- and long-term cellular load forecasting. The idea of using population dynamics together with relevant mobile cellular data, is of much broader scope than a specific scenario. Examining and quantifying the reductions in prediction error with mobile operator and road data on highways and urban scenarios would be the next step.

REFERENCES

- [1] O. Aouedi, V. A. Le, K. Piamrat, and Y. Ji, "Deep learning on network traffic prediction: Recent advances, analysis, and future directions," *ACM Computing Surveys*, vol. 57, no. 6, pp. 1–37, 2025.
- [2] W. Jiang, "Cellular traffic prediction with machine learning: A survey," *Elsevier Expert Systems with Applications*, vol. 201, pp. 117–163, 2022.
- [3] J. Gong, T. Li, H. Wang, Y. Liu, X. Wang, Z. Wang, C. Deng, J. Feng, D. Jin, and Y. Li, "KGDA: A knowledge graph driven decomposition approach for cellular traffic prediction," *ACM Transactions on Intelligent Systems and Technology*, vol. 15, no. 6, pp. 1–22, 2024.
- [4] J. Gong, Y. Liu, T. Li, J. Ding, Z. Wang, and D. Jin, "STTF: A spatiotemporal transformer framework for multi-task mobile network prediction," *IEEE Transactions on Mobile Computing*, 2025.
- [5] N. Vesselinova, "On the road to more accurate mobile cellular traffic predictions," *arXiv preprint arXiv:2305.15234*, 2023.
- [6] M. Amini, R. Stanica, and C. Rosenberg, "Where are the (cellular) data?" *ACM Computing Surveys*, vol. 56, no. 2, pp. 1–25, 2023.
- [7] T. Italia, "Telecommunications - SMS, Call, Internet - TN," 2015. [Online]. Available: <https://doi.org/10.7910/DVN/QLCABU>
- [8] C. Chen, K. Petty, A. Skabardonis, P. Varaiya, and Z. Jia, "Freeway performance measurement system: mining loop detector data," *Transportation research record*, vol. 1748, no. 1, pp. 96–102, 2001.
- [9] M. Gramaglia, P. Serrano, J. A. Hernández, M. Calderon, and C. J. Bernardos, "New insights from the analysis of free flow vehicular traffic in highways," in *2011 IEEE International Symposium on a World of Wireless, Mobile and Multimedia Networks*, 2011, pp. 1–9.
- [10] N. Vesselinova, "Admission control in mobile cellular networks: design, performance evaluation and analysis," Ph.D. dissertation, Universitat Politècnica de Catalunya, April 2012.
- [11] J. Guo, F. Liu, and Z. Zhu, "Estimate the call duration distribution parameters in GSM system based on KL divergence method," in *2007 International Conference on Wireless Communications, Networking and Mobile Computing*. IEEE, 2007, pp. 2988–2991.
- [12] E. A. Yavuz and V. C. Leung, "Modeling channel occupancy times for voice traffic in cellular networks," in *2007 IEEE International Conference on Communications*. IEEE, 2007, pp. 332–337.
- [13] D. Willkomm, S. Machiraju, J. Bolot, and A. Wolisz, "Primary users in cellular networks: A large-scale measurement study," in *2008 3rd IEEE Symposium on New Frontiers in Dynamic Spectrum Access Networks*, 2008, pp. 1–11.
- [14] L. Fang, X. Cheng, H. Wang, and L. Yang, "Mobile demand forecasting via deep graph-sequence spatiotemporal modeling in cellular networks," *IEEE Internet of Things Journal*, vol. 5, no. 4, pp. 3091–3101, 2018.
- [15] A. Palaios, M. Michalopoulou, J. Riihijärvi, and P. Mähönen, "When primary users whisper: A preliminary analysis on correlations of population-traffic dynamics," in *2014 9th International Conference on Cognitive Radio Oriented Wireless Networks and Communications (CROWNCOM)*. IEEE, 2014, pp. 19–25.
- [16] R. Becker, R. Cáceres, K. Hanson, S. Isaacman, J. M. Loh, M. Martonosi, J. Rowland, S. Urbanek, A. Varshavsky, and C. Volinsky, "Human mobility characterization from cellular network data," *Communications of the ACM*, vol. 56, no. 1, pp. 74–82, 2013.
- [17] C. Bergroth, O. Järv, H. Tenkanen, M. Manninen, and T. Toivonen, "A 24-hour population distribution dataset based on mobile phone data from Helsinki Metropolitan Area, Finland," *Scientific data*, vol. 9, no. 1, p. 39, 2022.
- [18] F. Ricciato, P. Widhalm, F. Pantisano, and M. Craglia, "Beyond the "single-operator, CDR-only" paradigm: An interoperable framework for mobile phone network data analyses and population density estimation," *Pervasive and Mobile Computing*, vol. 35, pp. 65–82, 2017.
- [19] J. Gong, Y. Liu, T. Li, H. Chai, X. Wang, J. Feng, C. Deng, D. Jin, and Y. Li, "Empowering spatial knowledge graph for mobile traffic prediction," in *Proceedings of the 31st ACM International Conference on Advances in Geographic Information Systems*, 2023, pp. 1–11.
- [20] X. Yin, G. Wu, J. Wei, Y. Shen, H. Qi, and B. Yin, "Deep learning on traffic prediction: Methods, analysis, and future directions," *IEEE Transactions on Intelligent Transportation Systems*, vol. 23, no. 6, pp. 4927–4943, 2021.
- [21] Y. Fang, S. Ergüt, and P. Patras, "SDGNet: A handover-aware spatiotemporal graph neural network for mobile traffic forecasting," *IEEE Communications Letters*, vol. 26, no. 3, pp. 582–586, 2022.
- [22] S. Zhao, X. Jiang, G. Jacobson, R. Jana, W.-L. Hsu, R. Rustamov, M. Talasila, S. A. Aftab, Y. Chen, and C. Borcea, "Cellular network traffic prediction incorporating handover: A graph convolutional approach," in *2020 17th Annual IEEE International Conference on Sensing, Communication, and Networking (SECON)*, 2020, pp. 1–9.
- [23] J. Singh, M. Götten, A. Ahrens, and S. Lochmann, "Simultaneous data transmission and sensor interrogation in a fiber optical sensor network," in *2022 IEEE 95th Vehicular Technology Conference:(VTC2022-Spring)*. IEEE, 2022, pp. 1–5.